are capable of reproducing all known trends for all nuclear spin–spin coupling constants in the series ethane–aminomethane–methanol–fluoromethane. For some of the coupling constants, primarily ^1J(C–H) and ^3J(H–H), the absolute values of the calculations are also very close to experimental values. Geminal coupling constants are a more difficult case. The one-bond coupling constants between the atom X (C, N, O, F) and the methyl carbon become increasingly more difficult to describe as the electronegativity of X increases. This is also true for the one-bond couplings between X and the proton, in analogy with earlier observations in simple hydrides.

The inclusion of correlation effects is of varying importance for different types of coupling constants. If we use the ratio Q(SECORD) = $-J$(SECORD)/J(CHF) as the measure of the importance of the correlation effects, and limit our interest to the average values of coupling constants for the staggered conformation, we can note two types of behavior. First, we have the coupling constants for which Q(SECORD) is always positive and roughly constant in the series of molecules. These are, ordered by decreasing Q(SECORD), given in parentheses: ^2J(C–H) (74%), ^2J(H–H) (48%), ^3J(H–H) (37%), ^1K(X–H) (29%), and ^1J(C–H) (28%). For these cases, we can also note that Q(CI) = $-J$(CI)/J(CHF), when available, is similar to Q(SECORD) though somewhat smaller. The second type of behavior is observed for ^1K(X–C) and ^2K(X–H). Considering these coupling constants to be a function of X, we find that the CHF values and the correlation corrections have trends of their own: both change sign somewhere along the series X = C–F, but the positions of the sign change do not coincide. Consequently, Q(SECORD) and Q(CI) vary strongly throughout the series of substituted methanes and become negative for both couplings in methanol, where the correlation contributions thus enhance the CHF results.

Several of the coupling constants show a strong dependence on conformation. Inclusion of the correlation corrections always has a moderating effect on this dependence. The modified Karplus relation, eq 2, is an excellent representation of the dihedral angle dependence of ^3J(H–H) along the HCXH path in ethane and methanol. In the case of aminomethane and methanol, the angular dependence of coupling constants along the subpaths to the HCXH path, originating at the methyl proton, i.e., ^1J(C–H) and ^2K(X–H), can also be described by eq 2. It would undoubtedly be interesting to see whether this observation could be confirmed experimentally for suitable rigid compounds.

Acknowledgment. This work has been supported by the Swedish Natural Science Research Council.

Ion–Molecule Radiative Association Reactions. A Statistical Phase Space Theory Model

Lewis M. Bass, Paul R. Kemper, Vincent G. Anicich, and Michael T. Bowers*

Contribution from the Department of Chemistry, University of California, Santa Barbara, California 93106. *Received November 20, 1980*

Abstract: A general model is presented for the application of statistical reaction rate theory to ion–molecule association reactions. A detailed mechanism which accounts for both collisional and radiative transitions is invoked and the formal solution of the resulting mathematical equations is discussed. A simplified working model is then developed and applied to the reaction CH_3^+ + HCN → CH_3·HCN^+. The theoretical predictions are compared with new experimental data reported here as well as that of McEwan et al. and Schiff and Bohme. The model is then used to provide the foundation for a critical discussion of previous work on ion–molecule association reactions.

I. Introduction

The importance of ion–molecule reactions in the chemistry of interstellar clouds has been firmly established.[1] Measurement of a significant number of rate constants for reactions of species of interstellar importance has been accomplished. These rate constants, usually measured at 300 K, have been very useful in modeling interstellar molecular abundances.[1] There remain, however, some serious gaps in information, particularly regarding synthesis of some of the larger species that have been observed. This manuscript addresses this point, particularly the role of radiative association and how this process can be modeled by using statistical rate theory.

McEwan et al.[2] have recently reported the results of an ICR (ion-cyclotron resonance) spectrometry study of reaction I.1 in

$$CH_3^+ + HCN \xrightarrow{k_{obsd}^{(2)}} CH_3{\cdot}HCN^+ \qquad (I.1)$$

the presence of He bath gas in the pressure range from 1×10^{-6} to 2×10^{-2} torr. They concluded that the observed reaction proceeds via two distinct pathways

$$CH_3^+ + HCN \xrightarrow{k_{RA}^{(2)}} CH_3{\cdot}HCN^+ + h\nu \qquad (I.2)$$

$$CH_3^+ + HCN + He \xrightarrow{k^{(3)}} CH_3{\cdot}HCN^+ + He \qquad (I.3)$$

where $k_{RA}^{(2)}$ is the bimolecular rate constant for radiative association and $k^{(3)}$ is the rate constant for three-body association. The results were interpreted in terms of the mechanism given in eq I.4a–c,

$$A^+ + B \underset{k_b}{\overset{k_f}{\rightleftharpoons}} (AB^+)^* \qquad (I.4a)$$

$$M + (AB^+)^* \xrightarrow{\beta k_c} AB^+ + M \qquad (I.4b)$$

$$(AB^+)^* \xrightarrow{k_r} AB^+ + h\nu \qquad (I.4c)$$

where A ≡ CH_3, B ≡ HCN, M = He, and the rate constants k_f, k_b, k_c, and k_r correspond to formation of the complex, back-dissociation of the complex, collisions of the complex with bath

(1) A. Dalgarno and J. H. Black, *Rep. Prog. Phys.*, **39**, 573 (1976); E. Herbst and W. Klemperer, *Phys. Today*, **29**, 32–39 (1976); *ibid.*, **26**, 505 (1973); W. T. Huntress, *Chem. Soc. Rev.* **6**, 295 (1977).

(2) M. J. McEwan, V. G. Anicich, W. T. Huntress, P. R. Kemper, and M. T. Bowers, *Chem. Phys. Lett.*, **75**, 278 (1980).

0002-7863/81/1503-5283$01.25/0

gas M, and stabilization via radiative emission, respectively, and β is the fraction of collisions with the bath gas which result in stabilization of the complex. Using the upper limits on k_f and k_s providewd by classical collision theory[3-5] and assuming that $\beta = 1$, these authors estimated $k_b \leq 2.5 \times 10^6$ s^{-1} and $k_r \leq 2 \times 10^5$ s^{-1}.

In this paper we present a theoretical analysis of this system based on the "phase space" model of statistical reaction rate theory.[6] This model has previously been successful in describing the three-body association reactions for formation of the proton-bound dimers of ammonia and methyl-substituted amines.[7]

The RRKM-QET formulation of statistical theory[8] has previously been applied to ion–molecule radiative association reactions by Woodin and Beauchamp[9] and by Herbst.[10] Herbst has also used statistical theory in canonical form to calculate thermally averaged rate constants directly.[11] Certain criticisms presented by Bates[12] have been addressed in Herbst's most recent work.[11b] The major advantage of the phase-space model over these other treatments is that angular momentum conservation is accounted for rigorously, allowing the centrifugal barrier, which plays an important role in ion–molecule collisions, to be dealt with explicitly. The rate constant for unimolecular dissociation is calculated as a function of energy and angular momentum, and the phenomenological rate is obtained by averaging over the appropriate distribution function. A more detailed comparison between the RRKM-QET formulation and the phase space model with regard to chemical activation systems has been presented previously.[7]

This paper is organized as follows. In section II, the experimental work and data analysis are discussed and compared with previous results reported by McEwan et al.[2] In section III, the details of the theoretical model, including the necessary assumptions and approximations, are presented. In section IV, the results of the calculations are presented and compared with the experimental results reported in section II. In section V, the implications of the model concerning ion–molecule association reactions in general are discussed.

II. Experimental Section

A. Experimental Data. The data presented in this paper were obtained by using a temperature-variable drift mode ion cyclotron resonance (ICR) spectrometer as described previously.[13] Reagent gas pressures above 10^{-4} torr were measured directly by using an MKS series 145 capacitance manometer. Lower pressures were measured by using an ionization gauge tube calibrated against the manometer. Ion drift times in the cell were measured by using the grid/trap plate pulsing method.[14] The experiments were done at a constant magnetic field of 10 kG. The marginal oscillator sensitivity at different frequencies was measured by using a "Q-spoiler" type standard signal.[15] Also, for reasons given below, it was necessary to sweep the marginal oscillator frequency to obtain the peak heights. The circuitry necessary to sweep the marginal oscillator frequency, including an appropriate frequency to voltage converter and a constant oscillation level control, will be described elsewhere.[16]

Methyl iodide was used as a source of CH_3^+ ions (rather than CH_4) in these experiments for two reasons. One, the weaker CH_3–I bond should allow formation of CH_3^+ ions with minimal internal energy. Second, we found that CH_4^+ ions reacted with HCN to give an ion at m/e 42$^+$, the nominal mass to charge ratio of the CH_3·HCN$^+$ condensation product. The rates for CH_3^+ and CH_4^+ reaction to form 42$^+$ were comparable; the CH_4^+ rate being slightly slower. In an attempt to avoid this interfering reaction, CH_3I was used as a source of CH_3^+ ions. Unfortunately the CH_3I^+ parent ion also reacted with the HCN to give 42$^+$. However, the large mass separation between the CH_3I^+ and other ions in the system allowed for quantitative double-resonance ejection of the CH_3I^+. Plots of ejection efficiency (ion intensity vs. ejection field strength) showed quantitative ejection could be obtained even at the highest pressures used. On the basis of these results it was decided to do the experiments using fixed magnetic field and double-resonance oscillator frequency to continuously eject the CH_3I^+ and to sweep the marginal oscillator detector frequency to observe the CH_3^+ and 42$^+$ ions.

The rate constant for the CH_3^+ + HCN reaction at 300 K was found to be 1.0×10^{-10} cm^3/s. The experimental scatter was $\pm 1 \times 10^{-11}$ cm^3/s, but the absolute uncertainty is probably $\pm 5 \times 10^{-11}$ cm^3/s. This value is in good agreement with that reported previously.[2] The He pressure dependence of the rate is shown in Figures 2 and 3. The rate constant increases from 1.0×10^{-10} cm^3/s at zero He pressure to 4.4×10^{-10} cm^3/s at 4.0×10^{-2} torr. A plot of rate constant vs. He pressure is linear to at least 4×10^{-2} torr. The slope of this line gives the three-body rate as $(2.7 \pm 0.1) \times 10^{-25}$ cm^6/s at low pressure (within the limits discussed later in this paper).

The Ne pressure dependence was also measured and the three-body rate determined to be $(3 \pm 0.3) \times 10^{-25}$ cm^6/s. The Langevin collision rate between 42$^+$ and Ne is 6.0×10^{-10} cm^3/s; for 42$^+$ and He it equals 5.7×10^{-10} cm^3/s. Thus the stabilization efficiencies of He and Ne are very nearly equal. Since a large difference in ionization potential between CH_3I and the bath gas was necessary (to avoid ionizing the bath gas), only He and Ne could be used.

The temperature dependence of the rate constant is shown in Figure 4. The rate constant decreases with increasing temperature, but the experimental scatter precludes assigning an exact functional dependence.

B. Experimental Analysis. In this section we briefly review the method used by McEwan et al.[2] to obtain values for k_b and k_r from the experimental data. Estimates of k_b and k_r will be made by analyzing the new data presented here in the same manner. This is done for two reasons: one, to provide a basis for comparison between previous work and that presented here; two, to point out explicitly the assumptions which are made in such an analysis. The validity and implications of these assumptions are discussed in the following sections.

Application of the steady-state hypothesis to $(AB^+)^*$ in reactions I.4 leads to equations II.1–3.

$$k_{obsd}^{(2)} = \frac{k_f(\beta k_c[M] + k_r)}{k_b + \beta k_c[M] + k_r} \quad \text{(II.1)}$$

$$k^{(3)} = \frac{k_f \beta k_c}{k_b + \beta k_c[M] + k_r} \quad \text{(II.2)}$$

$$k_{RA}^{(2)} = \frac{k_f k_r}{k_b + \beta k_c[M] + k_r} \quad \text{(II.3)}$$

Noting the increase in $k_{obsd}^{(2)}$ with added [He] for a given value of [HCN] and using eq II.2, McEwan et al.[2] estimated $k^{(3)}$ to be 5×10^{-25} cm^6/s. Plotting the present values of $k_{obsd}^{(2)}$ vs. [He] gave a linear plot up to at least 4×10^{-2} torr. From the slope of this line $k^{(3)}$ is estimated to be $(2.7 \pm 0.1) \times 10^{-25}$ cm^6/s. The methods are equivalent and are based on two assumptions: (1) that dissociation of the complex is much faster than stabilization in this pressure range; (2) that the rate constants in (I.4) are independent of pressure. Within the framework of these assumptions

$$k_{obsd}^{(2)} = k_{RA}^{(2)} + \frac{k_f \beta k_c}{k_b}[He] \quad \text{(II.4)}$$

and a linear plot of $k_{obsd}^{(2)}$ vs. [He] is expected. With the assumption that all A^+/B collisions result in complex formation, eq II.4 allows an upper limit to be placed on the ratio k_b/β by using the values of k_f and k_c calculated from collision theory ($k_f = 3.4 \times 10^{-9}$ cm^3/s; $k_c = 5.7 \times 10^{-10}$ cm^3/s).[3-5] The limit is calculated here to be 7.1×10^6 s^{-1}, as

(3) P. Langevin, *Ann. Chim. Phys.*, **5**, 245 (1905); G. Gioumousis and D. P. Stevenson, *J. Chem. Phys.*, **29**, 294 (1958); E. Vogt and G. H. Wannier, *Phys. Rev.*, **95**, 1190 (1954).
(4) T. Su and M. T. Bowers, *J. Chem. Phys.*, **17**, 309 (1975); L. Bass, T. Su, W. J. Chesnavich, and M. T. Bowers, *Chem. Phys. Lett.*, **34**, 119 (1975).
(5) W. J. Chesnavich, T. Su, and M. T. Bowers, *J. Chem. Phys.*, **72**, 2641 (1980).
(6) W. J. Chesnavich and M. T. Bowers, *J. Chem. Phys.*, **66**, 2306 (1977); *J. Am. Chem. Soc.*, **98**, 8301 (1976); W. J. Chesnavich, Ph.D. Thesis, University of California, Santa Barbara, CA, 1976.
(7) L. Bass, W. J. Chesnavich, and M. T. Bowers, *J. Am. Chem. Soc.*, **101**, 5493 (1979).
(8) P. J. Robinson and K. A. Holbrook, "Unimolecular Reactions", Wiley-Interscience, New York, 1972. W. Forst, "Theory of Unimolecular Reactions", Academic Press, New York, 1973.
(9) R. L. Woodin and J. L. Beauchamp, *Chem. Phys.*, **41**, 1 (1979).
(10) E. Herbst, *Ap. J.*, **205**, 94 (1976).
(11) (a) E. Herbst, *J. Chem. Phys.*, **70**, 2201 (1979); (b) E. Herbst, *Ap. J.*, **237**, 462 (1980); *J. Chem. Phys.*, **72**, 5284 (1980); *Ap. J.*, to be submitted for publication.
(12) D. R. Bates, *J. Phys.*, **12**, 4135 (1979).
(13) A. G. Wren, P. Gilbert, and M. T. Bowers; *Rev. Sci. Instrum.* **49**, 531 (1978); M. T. Bowers, P. V. Neilson, P. R. Kemper, and A. G. Wren, *Int. J. Mass. Spectrom. Ion Phys.* **25**, 103 (1978).
(14) T. B. McMahon and J. L. Beauchamp, *Rev. Sci. Instrum.*, **42**, 1632 (1971).
(15) P. R. Kemper and M. T. Bowers, *Rev. Sci. Instrum.* **48**, 1477 (1977).
(16) P. R. Kemper and M. T. Bowers, *Rev. Sci. Instrum.*, to be submitted for publication.

Table I. Theoretical and Experimental Rate Data in the ICR Pressure Regime at 300 K

		theory using k_r, s^{-1}			
	exptl	10^2	10^3	10^4	10^5
$10^{10}k_{RA}^{(2)}$, $cm^3\ mol^{-1}\ s^{-1}$	1.0 ± 0.2[a]	0.014[b]	0.12	0.78	4.7
$10^{25}k^{(3)}$, $cm^6\ mol^{-2}\ s^{-1}$	2.7 ± 0.1[c]	5.8[d]	5.4	4.4	2.7
		23[e]	22	20	13
10^5k_b, s^{-1}	<7.1[f]	3.3[d]	3.5	4.3	6.2
	<36[g]	4.2[e]	4.2	4.6	6.3

[a] This work; corresponds to $k_{obsd}^{(2)}$ in the limit of zero He pressure. [b] Calculated by using He pressure = 0 (thus, results are independent of β. [c] This work; assumed to correspond to the lower end of the experimental pressure regime shown in Figure 2 (about 10^{-3} torr). [d] Calculated by using He pressure = 10^{-3} torr and $\beta = 0.1$. [e] Calculated by using He pressure = 10^{-3} torr and $\beta = 0.5$. [f] This work; assuming $\beta = 0.1$. [g] This work; assuming $\beta = 0.5$.

compared to the value 2.5×10^6 reported by McEwan et al.[2]

A value for k_r is estimated as follows. At the helium concentration $[He]_{1/2}$ where $k_{obsd}^{(2)}$ is twice that at zero helium concentration, the radiative and collisional rates are equal, and two conditions must hold.

$$k_{RA}^{(2)} = k^{(3)}[He]_{1/2} \tag{II.5}$$

$$k_r = \beta k_c[He]_{1/2} \tag{II.6}$$

The low-pressure value of $k_{obsd}^{(2)}$ is used for $k_{RA}^{(2)}$ since at low-pressure collisional effects should be negligible. Using (II.5), $[He]_{1/2}$ is calculated and, together with a value for k_c from collision theory,[3-5] is used to find an upper limit on k_r (assuming $\beta = 1$) from (II.6). McEwan et al. estimate $k_r \leq 2 \times 10^5\ s^{-1}$, while from the present data we calculate $k_r \leq 2.1 \times 10^5\ s^{-1}$. An independent determination of β would also yield accurate values for k_b and k_r since k_b/β and k_rk_b are now known. Unfortunately this cannot be done with the present experiment. A summary of the rate constant values calculated above is given in Table I along with those predicted by the theory developed in the next section.

III. Theoretical Analysis

In subsection III.A the general, detailed mechanism corresponding to reaction scheme I.4 is presented. It will be seen that there is insufficient information on the $CH_3^+ + HCN$ system to warrant actual computations on the basis of this detailed mechanism. However, the formal solution of the problem will be presented, as this provides a framework for understanding the assumptions necessary to obtain a reasonable model which is applicable to the data available for the $CH_3^+ + HCN$ system. In subsection III.B we discuss the final working model which is used for the calculations reported here. In subsection III.C a brief review of the phase space theory formalism used in our calculations is given.

A. General Model. If reaction scheme I.4 is considered on a microscopic level, then the following reaction steps given in eq III.1a–c must be included,

$$A^+ + B \underset{k'_b(i)}{\overset{k_fF(i)}{\rightleftharpoons}} AB^+(i) \tag{III.1a}$$

$$AB^+(i) + M \underset{k_cP_c(j,i)}{\overset{k_cP_c(i,j)}{\rightleftharpoons}} AB^+(j) + M \tag{III.1b}$$

$$AB^+(i) \xrightarrow{k'_r(i,j)} AB^+(j) + h\nu \tag{III.1c}$$

where $F(i)$ is the probability that $CH_3{\cdot}HCN^+$ is initially formed in state i, $k'_b(i)$ is the microscopic rate constant for dissociation from state i back to reactants, k_c is the total rate constant for collisions between AB^+ and M, $P(i,j)$ is the probability that AB^+ in state i will undergo a transition to state j upon collision with M, $k'_r(i,j)$ is the rate constant for AB^+ initially in state i to undergo a radiative transition to state j, and the subscripts i and j represent any parameters necessary to define the state of AB^+.

Note that k_f has the same meaning in (III.1a) as in (I.4a)—it is the total rate constant for formation of AB^+ complex. In the second step in the mechanism collision-induced transitions between states are accounted for in detail. These transitions may be activating or deactivating or may involve two active or two inactive states. The important difference between mechanisms I.4 and III.1 is that in (I.4) the fact that collisional and radiative processes do not necessarily lead directly to stabilization has been ignored.

The phenomenological rate constants in scheme I.4 are related to the microscopic rate constants in (III.1) and the steady-state concentrations of $AB^+(i)$ by eq III.2a–c,

$$k_b = \sum_i k'_b(i)P_{ss}(i) \tag{III.2a}$$

$$\beta = \sum_{i=\text{active}} P_{ss}(i) \sum_{j=\text{inactive}} P_c(i,j) \tag{III.2b}$$

$$k_r = \sum_{i=\text{active}} P_{ss}(i) \sum_{j=\text{inactive}} k'_r(i,j) \tag{III.2c}$$

where $P_{ss}(i)$ is the steady-state distribution function for $(AB^+)^*$, given by eq III.3 and $[(AB^+)^*]$ is the total concentration of excited

$$P_{ss}(i) = \frac{[AB^+(i)]}{[(AB^+)^*]} \tag{III.3}$$

AB^+. These equations can be solved for k_b, β, and k_r which can then be used in eq II.1–3 to obtain $k_{obsd}^{(2)}$, $k^{(3)}$, and $k_{RA}^{(2)}$.

The steady-state concentrations of $AB^+(i)$ can be evaluated by applying the steady-state hypothesis to the mechanism in (III.1). This yields, for each state i

$$k_fF(i)[A^+][B] + \sum_j [AB^+(j)]\{k_c[M]P_c(j,i) + k'_r(j,i)\} = [AB^+(i)]\{k'_b(i) + \sum_j k_r(i,j) + k_c[M]\sum_j P_c(i,j)\} \tag{III.4}$$

Due to the cross terms involving $P_c(i,j)$ and $k'_r(i,j)$ the expression in (III.4) actually represents a system of coupled equations which must be solved simultaneously for the steady-state concentrations.[17] Note that the neutral collision gas concentration enters explicitly into eq III.4. Thus the steady-state concentrations are dependent on the pressure. Accordingly, all the phenomenological rate constants calculated from eq III.2 and II.1–II.4 may be pressure dependent.

Solution of Eq III.4 by various methods has been discussed by Tardy and Rabinovitch[18] for the case in which there are no radiative processes. This method is too complex to warrant application to the present case or to ion–molecule reactions in general, due to the largely unknown nature of $P_c(i,j)$ and $k'_r(i,j)$. Although a number of authors[19] have discussed various forms for $P_c(i,j)$, these have dealt only with energy transfer, not angular momentum transfer. In using the phase space model for $k'_b(i)$, both of these variables must be accounted for explicitly in the collisional transition probability matrix. Thus, even for the apparently simple mechanism in eq I.4, the problem becomes considerably more complex when considered on a microscopic level. The assumptions which are needed to develop a reasonable working model applicable to the present case must be understood in relation to the detailed model presented here. This will be done in the following section.

B. Simplified Model. In terms of the detailed mechanism presented in subsection A, the following assumptions result in a reasonable model which is applicable to the $CH_3^+ + HCN$ system: (1) the rate constant k_f for formation of excited AB^+ is given by classical collision theory;[3-5] (2) the rate constant k_c for AB^+/M collisions is given by classical collision theory;[3-5] (3) the fraction β is independent of the internal state of AB^+ while the remaining fraction of AB^+/M collisions are purely elastic; (4) radiative transitions between active states are negligible and the rate constant k_r for radiative stabilization is independent of the internal state of AB^+; (5) the rate constant k_b for dissociation of AB^+ back to reactants is a function of the energy E and angular momentum J of the AB^+ complex and is determined by the orbiting transition

(17) The fact that collisional processes should be considered in detail and that a set of coupled equations results has previously been noted by Bates in ref 12.

(18) D. C. Tardy and B. S. Rabinovitch, *Chem. Rev.*, 77, 369 (1977).

(19) See ref 18 and references therein.

state in the long-range part of the ion–molecule interaction potential. Note that assumptions 1 and 5 satisfy the principle of microscopic reversibility since collision theory uses the orbiting transition state to calculate k_f. Assumptions 3 and 4 can be written in terms of eq III.2 as

$$\sum_{j=\text{inactive}} P_c(i,j) = \text{constant} = \beta \text{ for all active i} \quad \text{(III.5)}$$

$$\sum_{j=\text{inactive}} k'_r(i,j) = \text{constant} = k_r \text{ for all active i} \quad \text{(III.6)}$$

Note that assumptions 3 and 4 probably are not realistic representations in the sense that these stabilization rates are, in principle, expected to vary with the internal state of the excited species. However, over a limited range of internal energies these rates may be treated in an average sense in order to allow the model to be tested on the level of a first approximation. Comparison between theory and experiment can then be used to estimate the values of β and k_r required to bring the model into agreement with the experimental data. It is important to note here that the values thus obtained for β and k_r are by no means intended to be definitive determinations of these quantities. Instead, these estimates are intended to provide a rough indication of the range of values expected for these quantities if they are not treated in an average sense. Hence, examination of the estimates obtained here may be used as a guide in modeling these steps in greater detail and in deciding if such a model is, in fact, likely to prove fruitful.

Using the above assumptions, the mechanism becomes eq III.7a–c.

$$A^+ + B \underset{k'_b(E,J)}{\overset{k_f F(E,J)}{\rightleftharpoons}} (AB^+)^* \quad \text{(III.7a)}$$

$$(AB^+)^* + M \xrightarrow{\beta k_c} AB^+ + M \quad \text{(III.7b)}$$

$$(AB^+)^* \xrightarrow{k_r} AB^+ + h\nu \quad \text{(III.7c)}$$

The collision theory[3-5] values for k_f and k_c are 3.4×10^{-9} and 5.7×10^{-10} cm^3 molecule^{-1} s^{-1}, respectively. The stabilization efficiency for He is expected to be somewhere in the range from 0.1 to 0.5.[20] Calculations were performed using stabilization efficiencies of 0.1, 0.3, 0.5, and 1.0. The rate constant for radiative emission is largely unknown, especially since the nature of the transition is unknown (i.e., vibrational or electronic). For vibrational transitions $k_r \approx 10^2$–10^3 s^{-1} while for electronic transitions $k_r \geq 10^5$–10^6 s^{-1}. We have performed a series of calculations varying k_r by orders of magnitude from 10^2 to 10^5 s^{-1}. The calculation of both $F(E,J)$ and $k'_b(E,J)$ are carried out using statistical phase space theory and are discussed in the following subsection.

With the assumptions listed above the steady-state expression in eq III.4 now becomes eq III.8 which leads to eq III.9 and III.10,

$$k_f F(E,J)[A^+][B] = [AB^+(E,J)]\{k'_b(E,J) + k_r + \beta k_c[M]\} \quad \text{(III.8)}$$

$$P_{ss}(E,J) = \frac{\dfrac{F(E,J)}{k'_b(E,J) + k_r + \beta k_c[M]}}{\displaystyle\int_{E_0}^{\infty} dE \int_0^{J_{max}} dJ \frac{F(E,J)}{k'_b(E,J) + k_r + \beta k_c[M]}} \quad \text{(III.9)}$$

$$k_b = \int_{E_0}^{\infty} dE \int_0^{J_{max}} dJ k'_b(E,J) P_{ss}(E,J) \quad \text{(III.10)}$$

where E_0 is the zero-point energy difference between AB^+ and separated fragments as shown in Figure 1 and J_{max} is the maximum J for which an $A^+ + B$ collision pair can overcome the centrifugal barrier at at given E.[6,7] Note that the sum over states i has been changed to a double integral over E and J since these are treated as continuous variables in the classical phase phase model. Equations II.1–3 are evaluated by using k_b given by eq III.10.

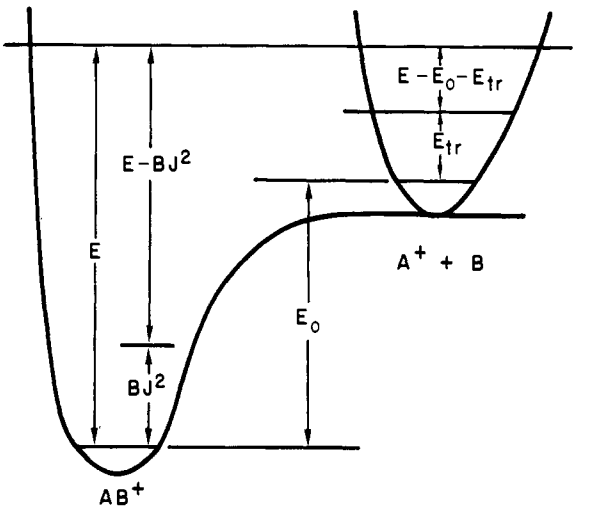

Figure 1. Schematic potential energy surrface showing energies of interest. See text for discussion.

C. Statistical Theory Evaluation of $F(E,J)$ and $k'_b(E,J)$. Consider the unimolecular reaction in eq III.1a to be described in terms of motion along a potential energy surface from the reactant region of the surface to the product region. For a given set of initial conditions classical dynamics may be used to determine the trajectory of the system's representative point along the potential energy surface. Selection of a representative sampling of initial conditions and determination of the corresponding trajectories provides the basis for the calculation of the rate constant by using classical dynamics.[21] Statistical rate theory is based on two assumptions: (1) that there exists a dividing surface, or transition state, somewhere in the system phase space such that all reactive trajectories cross this surface once and only and all nonreactive trajectories do not cross this surface at all; (2) subject only to restrictions imposed by conservation of energy and angular momentum all reactant states are populated uniformly and independently of the method of initial preparation. The second assumption is usually called the quasi-equilibrium or energy randomization hypothesis. Together, these two assumptions allow the reactive flux from reactants to products to be equated to the equilibrium flux at the transition state.

For the ion–molecule system discussed here the transition state is assumed to lie at the centrifugal barrier determined by the long-range ion-induced dipole term in the interaction potential. Since this barrier typically corresponds to relatively large ion–molecule separations (~5–20 Å), the transition state resembles two separated fragments, each with its own angular momentum and internal energy. The relative motion of the two fragments with respect to each other gives rise to an orbital angular momentum and a relative translational energy which must also be considered in applying the conservation laws.

This problem has been discussed in detail by Chesnavich and Bowers[6] for the dissociation of a spherical top species to form pairs of polyatomic fragments of various symmetries. In this work we treat CH_3·HCN^+ as a spherical top insofar as its rotational energy and angular momentum is concerned. The fragments are treated as a spherical (CH_3^+) and linear (HCN) pair. Chesnavich and Bowers have shown that the errors introduced by treating prolate and oblate symmetric tops as spherical tops will generally be small.[6]

(20) R. D. Cates and M. T. Bowers, *J. Am. Chem. Soc.*, **102**, 3994 (1980). These authors estimate $\beta = 0.31 \pm 10\%$ for helium used as a stabilizer with the excited proton-bound dimer of trimethylamine. Considering that β may vary from system to system we have chosen the range 0.1–0.5 to use in this work.

(21) See, for example: (a) D. L. Bunker and W. L. Hase, *J. Chem. Phys.* **59**, 4621 (1973); (b) W. L. Hase in "Dynamics of Molecular Collisions", Part B, W. H. Miller, Ed., Plenum Press, 1976, pp 121–169, and references therein.

(22) See, for example: W. J. Chesnavich and M. T. Bowers in "Gas Phase Ion Chemistry", Vol. I, M. T. Bowers, Ed., Academic Press, 1979, pp 119–153. See also the chapter by P. Pechukas in ref 21b.

Table II. Parameters Used in Calculations

	CH_3^+	HCN	$CH_3 \cdot HCN^+$
ν_i[a]	3100 (2)	3300 (1)	3400 (1)
	3000 (1)	2100 (1)	3000 (3)
	1200 (2)	700 (2)	2250 (1)
	575 (1)		1450 (2)
			1375 (1)
			1050 (2)
			925
			625 (2)
			325 (2)
B[b]	7.60	1.478	0.737
σ[c]	6	1	3
E_0[d]		98	

[a] Vibrational frequencies in cm^{-1} (degeneracy in parentheses). All frequencies rounded to nearest 25 cm^{-1}. [b] Rotational constant in cm^{-1}. [c] Symmetry number. [d] Zero-point energy difference (see Figure 1) in kcal/mol.

The resulting expression for the flux of $A^+ + B$ collision pairs through the centrifugal barrier to form a collision complex with energy E and angular momentum J is

$$\Phi(E,J) = (2J/h)\int_{E^*_{tr}}^{E} dE_{tr}\Gamma(E_{tr},J)\rho_v(E - E_0 - E_{tr}) \qquad (III.11)$$

where h is Planck's constant, $\Gamma(E_{tr},J)$ is the rotational-orbital sum of states for the fragments with translational-rotational energy E_{tr} and angular momentum J, $\rho_v(E - E_0 - E_{tr})$ is the vibrational density of states of the fragments at vibrational energy $E - E_0 - E_{tr}$, E_0 is the difference in zero-point energies between the fragments and the $CH_3 \cdot HCN^+$ complex, and E^*_{tr} is the minimum translational-rotational energy for which the fragments can overcome the centrifugal barrier at angular momentum J. The flux inside the integral in (III.11) pertains to a given value of J_z, the projection of J on an external axis. The $2J$ classical degeneracy is included to account for the full range of values possible for J_z.

According to the principle of microscopic reversibility the flux in eq III.11 must equal the flux of trajectories leading from AB^+ to fragments, which is given by expression III.12

$$(2J)^2 k'_b(E,J)\rho(E - BJ^2) \qquad (III.12)$$

where $k'_b(E,J)$ is the rate constant for dissociation, $\rho(E - BJ^2)$ is the vibrational density of states of the $CH_3 \cdot HCN^+$ complex with vibrational energy $E - BJ^2$, and B is the geometric mean rotational constant of AB^+ (yielding the classical rotational energy as BJ^2). The $(2J)^2$ factor in (III.12) arises from the degeneracies associated with the projection of J on an internal and an external axis for a spherical species. Equating (III.11) and (III.12) leads to the phase space theory expression for $k'_b(E,J)$[6]

$$k'_b(E,J) = \frac{\int_{E^*_{tr}}^{E} dE_{tr}\Gamma(E_{tr},J)\rho_v(E - E_0 - E_{tr})}{2Jh\rho(E - BJ^2)} \qquad (III.13)$$

The distribution function $F(E,J)$ for formation of the $CH_3 \cdot HCN^+$ complex is obtained by weighting the flux in (III.11) by the thermal energy distribution and then normalizing[7]

$$F(E,J) = \frac{e^{-E/k_BT}\Phi(E,J)}{\int_{E_0}^{\infty} dE e^{-E/k_BT}\int_0^{J_{max}} dJ\Phi(E,J)} \qquad (III.14)$$

where k_B is Boltzmann's constant.

Evaluation of the sums and densities of states required in the above equations involves the vibrational frequencies and rotational constants of the CH_3^+, HCN and $CH_3 \cdot HCN^+$ species. These parameters are discussed in Appendix B and summarized in Table II.

IV. Results

The calculations described in the preceding section were performed for a series of values of k_r (10^2, 10^3, 10^4, 10^5 s^{-1}) and β (0.1, 0.3, 0.5, 1.0). Since the theoretical results at the low-pressure end of the experimental regime are relatively insensitive to β (because the collisional stabilization step is essentially negligible), these results can be used to obtain an order-of-magnitude estimate of k_r. Table I summarizes the dependence of the theoretical results on the value of k_r and β at a helium pressure of 10^{-3} torr (roughly corresponding to the lower limit of the experimental pressure regime). Note that the calculated value of $k_{RA}^{(2)}$ is quite sensitive to changes in k_r, while the calculated value of $k^{(3)}$ is most sensitive to changes in β. This is expected since k_r has a direct effect on $k_{RA}^{(2)}$ while β (by determining k_s) has a direct effect on $k^{(3)}$. More subtle effects, arising from the dependence of the distribution function $P_{ss}(E,J)$ on k_r and β, are responsible for the relatively weak dependence of k_b on these parameters. From the data in Table I is is clear that good agreement between theory and experiment for $k_{obsd}^{(2)}$ is obtained only for $k_r \approx 10^4$ s^{-1}. The value of k_r which yields the best agreement with the experimental value of $k_{obsd}^{(2)}$ in Table I is estimated by interpolation to be $k_r = 1.4 \times 10^4$ s^{-1}. For the remainder of this work, therefore, all theoretical results reported will be those obtained by using $k_r = 1.4 \times 10^4$ s^{-1}. This estimate is expected to be accurate to within about a factor of 5.

A comparison of theory and experiment at room temperature is shown in Figure 2 for the ICR pressure range and in Figure 3 for the pressure range of flow tube measurements. The data points shown in Figure 2 are those obtained from the experimental work reported here; the point in Figure 3 is that measured by Schiff and Bohme.[23] In both figures theoretical curves are shown

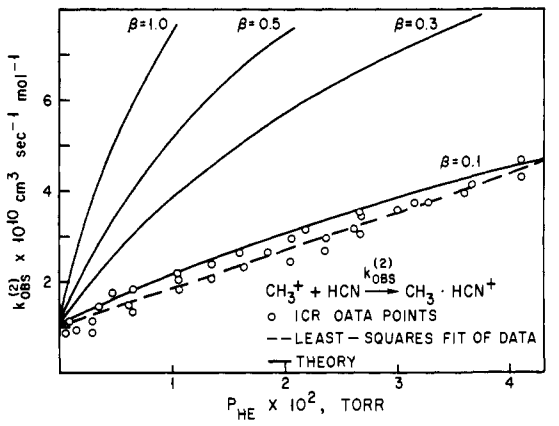

Figure 2. Comparison of theoretical and experimental values of $k_{obsd}^{(2)}$ in the ICR pressure range. Theoretical curves use $k_r = 1.4 \times 10^4$ s^{-1} and four values of β as indicated. Experimental results are those reported here.

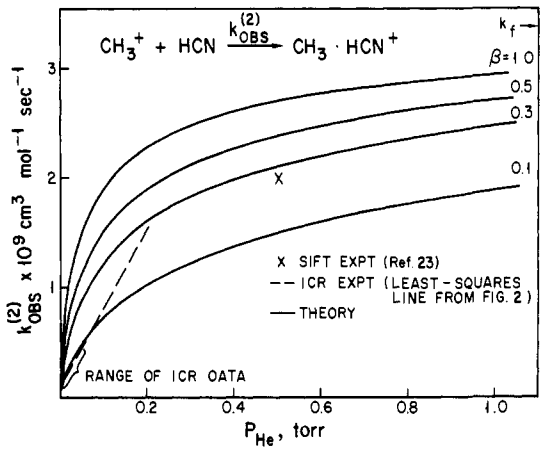

Figure 3. Comparison of theoretical and experimental values of $k_{obsd}^{(2)}$ in the pressure range up to 1.2 torr. Broken line corresponds to least-squares fit of ICR data in Figure 2; SIFT point is from ref 23; theoretical curves use $k_r = 1.4 \times 10^4$ s^{-1} and four values of β as indicated.

(23) H. I. Schiff and D. K. Bohme, *Ap. J.*, **232**, 740 (1979).

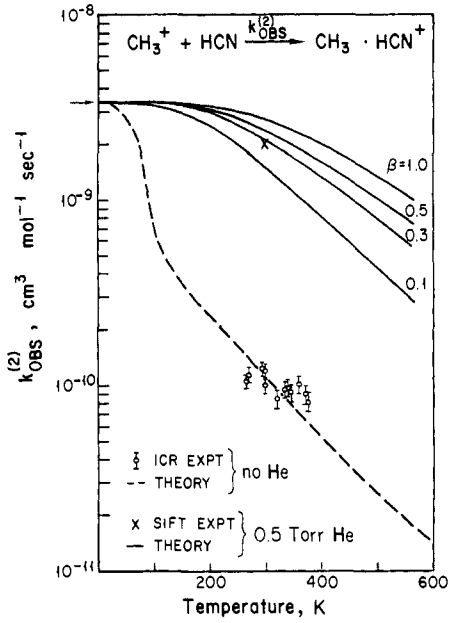

Figure 4. Predicted temperature dependence of $k_{obsd}^{(2)}$ in the limit of zero helium pressure (---) and at 0.5 torr He (—) for four different values of β as indicated. ICR points from this work correspond to zero pressure; SIFT point from ref 23 corresponds to 0.5 torr.

for β = 0.1, 0.3, 0.5, and 1.0. The variation of β with pressure is a complicated function of the collisional transition probability matrix and the specific pressure range of interest.[24] The results shown in Figures 2 and 3 indicate that good agreement between theory and experiment can be obtained if β increases from about 0.1 at low pressures to about 0.3 in the region near 0.5 torr.

An interesting point to note here is that even for the case β = 1.0 the theoretical model predicts that $k_{obsd}^{(2)}$ does not reach the collision theory[3-5] value until pressures substantially greater than 1 torr are reached. Thus, the system is not expected to exhibit "saturated" kinetics in the range of the flow tube measurement at 0.5 torr. This will be discussed more fully in the following section.

The predicted temperature dependence of $k_{obsd}^{(2)}$ is shown in Figure 4 for the limiting case of zero helium pressure and for a pressure of 0.5 torr. The experimental data shown were obtained from ICR measurements performed in the absence of helium gas and in the HCN pressure range from 0 to about 5×10^{-5} torr. Collisional stabilization of the excited complex by collisions with HCN was ignored in the calculations. This is justified by the fact that stabilization via He collision does not have an appreciable effect on $k_{obsd}^{(2)}$ until pressures upward of about 10^{-3} torr. HCN would thus have to be about twenty times as effective a stabilizer as He in order to have a significant effect at 5×10^{-5} torr.

The theoretical curves in Figure 4 show very good agreement with the magnitude of the experimental data, although the temperature dependence predicted at zero pressure is somewhat steeper than that shown by the ICR data. It would be interesting to obtain experimental measurements of $k_{obsd}^{(2)}$ at helium pressure of 0.5 torr to compare with the theoretical curves in Figure 4.

Finally, we would like to note that k_r and β could be varied more systematically in order to optimize the agreement between theory and experiment in the cases just discussed. However, at this point we do not feel that there is much to gain from a study such as this. We believe that the results presented here are sufficient to show that the CH_3^+ + HCN system can be modeled by using statistical phase-space theory and reasonable values for all necessary parameters. Further theoretical work may prove fruitful in modeling the radiative and collisional steps more completely, i.e., taking into consideration the microscopic parameters $k'_r(i,j)$ and $P_c(i,j)$ in eq III.1.

(24) D. C. Tardy and B. S. Rabinovitch, *J. Chem. Phys.*, **48**, 1282 (1968); M. Hoare, *ibid.*, **38**, 1630 (1963).

V. Discussion

The application of statistical theory to ion–molecule radiative association reactions as presented in this paper is based upon the assumptions listed in section III. The relatively good agrement between theory and experiment suggests that these assumptions are at least approximately valid for the CH_3^+ + HCN system. We will begin this section with a more detailed discussion of these assumptions and their implications.

The first two assumptions in section III.B state that the rate constants k_f and k_c are both given by classical collision theory. It is generally well established that ion–molecule collision rates are determined by the long-range part of the ion–molecule potential.[25,26] The classical Langevin treatment[3] is valid when the charge-induced dipole term totally dominates the potential. Either ADO theory[4] or the more recently developed variational transition-state approach[5] may be used to account for neutrals which have strong permanent dipole moments. Contributions from higher order terms (charge–quadrupole, induced dipole–induced dipole) are expected to be negligible for a neutral such as HCN which has a permanent dipole moment.

Since k_f is the rate constant for formation of the excited AB^+ intermediate, use of the collision theory value requires the additional assumption that all CH_3^+/HCN collisions do, in fact, result in complex formation. Although some attempt may be made to estimate k_f directly from high-pressure rate data, this approach is not valid, as we will show later on when discussing "high"- and "low"-pressure regimes. If not all collisions lead to complex formation, collision theory will still provide a valid upper limit on k_f.

The third assumption in section III.B states that the rate constant for stabilization of the excited intermediate via collision with bath gas is independent of the internal state of the intermediate. Thus, the stabilization rate constant can be expressed as the product of the collision rate constant, k_c, and the stabilization efficiency, β, which is independent of pressure and temperature. Since the only dissociation channel available to the complex is back-reaction to the ion–molecule reactant pair, stabilization occurs when sufficient energy is removed from the complex so that back-dissociation can no longer occur.

It is unlikely that β is, in reality, independent of temperature and pressure. This should be kept in mind when attempting to estimate β from experimental data. For instance, Smith and Adams[27] suggested a method for estimating β from the high-pressure association rate. They then used this value of β in conjunction with their low-pressure rate data. Even if the high-pressure estimate of β is accurate (which Bates[12] has questioned and which we discuss later), this value of β is not necessarily applicable to the low-pressure regime. Further, there is no simple relation between the high- and low-pressure values of β which may be used to predict one if the other is known.

Each of the curves shown in Figures 2 and 3 was calculated by using a constant value of β throughout the pressure range. These curves give some indication of the behavior that may be predicted by a more sophisticated theory which accounts explicitly for the pressure dependence of β. The exact shape of such a curve depends on the particular pressure range in which β shifts from its low-pressure to its high-pressure value. Thus, although we can say that the present study indicates that the experimental results for the CH_3^+ + HCN system are consistent with the theoretical model if β is in the range from 0.1 to 0.3, we cannot conclude that a more detailed model would necessarily match the experimental data over the entire pressure range. This can only be checked by actually implementing such a model and examining the results. In any case, the use of an average value of β in a model

(25) T. Su and M. T. Bowers, "Interactions Between Ions and Molecules", P. Ausloos, Ed., Plenum Press, New York, 1975, pp 163 ff. D. K. Bohme, *ibid.* G. I. Mackay and D. K. Bohme, *Int. J. Mass Spectrom. Ion. Phys.*, **26**, 327 (1978). See chapter by T. Su and M. T. Bowers in ref 22.

(26) W. J. Chesnavich, T. Su, andd M. T. Bowers, "Kinetics of Ion-Molecule Reactions", P. Ausloos, ed., Plenum Press, New York, 1979, pp 31–35, *J. Chem. Phys.*, **71**, 7308 (1980).

(27) D. Smith and N. G. Adams, *Chem. Phys. Lett.*, **54**, 535 (1978).

such as that presented here will tend to obscure the pressure dependence of the results.

The fourth assumption in section III.B states that k_r is independent of the internal state of the excited intermediate and that all radiative processes lead directly to stabilization. Thus k_r becomes the rate constant for radiative stabilization, not for radiative transitions, in general. Although k_r is expected to be energy dependent for any realistic system, the use of an average value throughout the energy range of interest is probably not a bad approximation in this case. About 90% of the ion–molecule activating reactions occur with total energy less than 0.3 eV above the reactant pair (for a more detailed discussion of the ion-molecule activation process, see ref 7). Thus, 90% of the complexes formed have energies in the range from 4.2 to 4.5 eV above the zero-point level of the CH_3·HCN^+ complex. Inspection of the data presented by Woodin and Beauchamp[9] for the energy dependence of the radiative decay rates in a number of species indicates that the variation of k_r over the range from 4.2 to 4.5 eV will probably be less than about 25%. Thus, the assumption of a constant value throughout this energy range is certainly consistent with the use of the present model to obtain a rough order-of-magnitude estimate of k_r. More detailed treatment of the radiative process, such as that presented by Woodin and Beauchamp,[9] is probably the next step in modeling and understanding ion–molecule radiative association in general.

The fifth assumption in Section III.B states that the rate constant for dissociation of CH_3·HCN^+ back to reactants can be calculated from statistical phase space theory. This requires that the two assumptions in Section III.C are valid: the rate of reaction must be governed by an appropriate transition state and the CH_3HCN^+ intermediate must reach a state of quasi-equilibrium prior to dissociation. The success of phase space theory in describing a number of similar ion-molecule systems[7,28] suggests that such a treatment should be applicable to the present case as well. Although in some cases involving excited ions in energy regimes substantially greater than the decomposition thresholds it has been shown that both tight and orbiting transition states must be included along the reaction coordinate,[28] we know of no cases for which the thermal energy ion–molecule collision process and the corresponding back-dissociation are not adequately described by the orbiting transition state alone. The experimental estimate that the lifetime of the CH_3·HCN^+ intermediate is 10^{-6} s indicates that there is certainly sufficient time for quasi-equilibrium to occur prior to dissociation. On the basis of the good agreement between theory and experiment presented in Section IV it is reasonable to conclude that the basic assumptions of transition-state theory are met, at least to a good first approximation, for the CH_3·HCN^+ dissociation process. There is probably not much to be gained from refinements in this aspect of the problem until the much greater uncertainties in k_r and β are addressed.

The assumptions discussed above are primarily concerned with the detailed microscopic mechanism in (III.1). On the basis of these assumptions the mechanism is simplified to that in (III.7), the major simplifications being that k_r and β are assumed to be independent of pressure. The analysis of experimental data is usually based on the simpler phenomenological mechanism in (I.4), in which the rate contant k_b is also taken to be independent of pressure. The present model can be used as a guide in discussing the reliability of various methods of experimental analyses in view of the fact that the various rate contants may, in fact, be pressure dependent. It should be kept in mind that the present model accounts explicitly for the pressure dependence of k_b but not of β or k_r. Hence, although this model may be used to gain some insight into the behavior expected if β and k_r do vary, this is no substitution for a model which simultaneously accounts for the pressure dependence of k_b, k_r, and β.

Before discussing the complications introduced by pressure-dependent rate constants, we should say a few words about the simple mechanism in (I.4) since this mechanism has sometimes

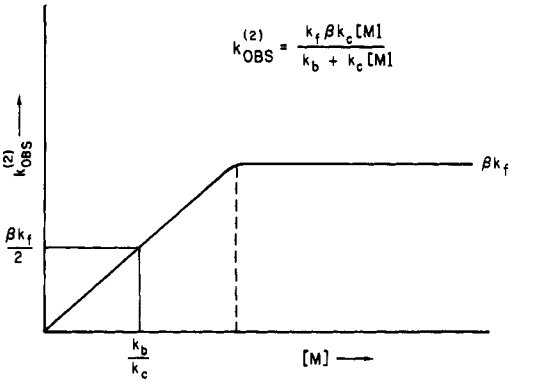

Figure 5. Schematic diagram of $k_{obsd}^{(2)}$ vs. [M] as presented in Figure 1 of ref 27.

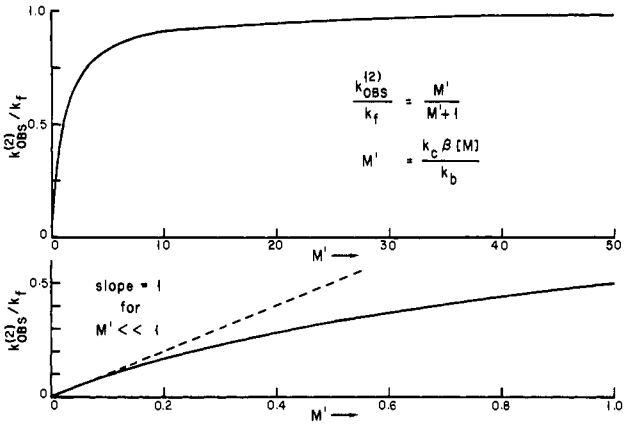

Figure 6. Plot of $k_{obsd}^{(2)}/k_f$ vs. reduced pressure M′, assuming the kinetics described by eq V.2.

been misinterpreted in the literature. For instance, Smith and Adams have applied this mechanism to simple three-body association and used a curve similar to that shown in Figure 5 to illustrate the behavior predicted by the mechanism in (I.4).[29] Note that these authors incorrectly assumed that the fraction, $1 - \beta$, of bath gas collisions which do not result in stabilization will result in collision-induced dissociation.[12] Hence the expression for $k_{obsd}^{(2)}$ becomes eq V.1, and at high pressures $k_{obsd}^{(2)}$ should approach

$$k_{obsd}^{(2)} = \frac{k_f k_c \beta [M]}{k_b + k_c [M]} \qquad (V.1)$$

βk_f. At the pressure $[M] = k_b/k_c$ substitution into (V.1) yields $k_{obsd}^{(2)} = {}^1/_2 \beta k_f$. Hence this pressure corresponds to the solid line in Figure 5 and not to the dashed line, as was indicated by Smith and Adams.[27]

The incorrect labeling of the pressure $[M] = k_b/k_c$ depicts graphically the assumption used earlier by Bohme et al.[30] that "saturation" corresponds roughly to the pressure at which the collision frequency is equal to the lifetime of the complex with regard to unimolecular decomposition.

The curve in Figure 5 is misleading in that it shows much too sharp a transition from low-pressure to high-pressure kinetics. The correct kinetic expression for $k_{obsd}^{(2)}$ can be written as eq V.2,

$$\frac{k_{obsd}^{(2)}}{k_f} = \frac{M'}{1 + M'} \qquad (V.2)$$

where M′ is the reduced pressure given by eq V.3. This equation

$$M' = \frac{k_c \beta [M]}{k_b} \qquad (V.3)$$

(28) W. J. Chesnavich, L. Bass, T. Su, and M. T. Bowers, *J. Chem. Phys.*, **74**, 2228 (1981).

(29) See Figure 1 in ref 27. Note that the symbols β, $k_{obsd}^{(2)}$, k_b, k_f, and k_c used here correspond, respectively, to f, $k_c[M]$, $1/\tau_d$, k_1, and k_2 used in ref 27.

(30) D. K. Bohme, D. B. Dunkin, F. C. Fehsenfeld, and E. E. Ferguson, *J. Chem. Phys.*, **49**, 5201 (1968).

leads to the curve shown in Figure 6, from which it is apparent that the transition from low to high-pressure kinetics occurs over a presure change of a few orders of magnitude. This can be seen algebraically by considering the definitions of low and high pressure which follow from mechanism I.4 and eq V.2.

$$\text{low pressure: } M' << 1 \quad \text{(V.4a)}$$

$$\text{high pressure: } M' >> 1 \quad \text{(V.4b)}$$

Even the most liberal interpretation of the inequalities in eq V.4 requires $M' \leq 0.1$ for eq V.4a to hold the $M' \geq 10$ for eq V.4b to hold. Thus, the transition region must correspond to a pressure change of 2 orders of magnitude at the very least, with 4 orders of magnitude not being unreasonable.

In the previous work reported by Smith and Adams[27] values for the ratio β/k_b were evaluated from the linear, low-pressure part of the $k_{obsd}^{(2)}$ vs. [M] curve and are therefore correct. Values for β were estimated from data assumed to correspond to "saturated" pressures. These values are not correct, even if saturation did in fact occur, because these estimates were based on the assumption that $k_{obsd}^{(2)} \rightarrow \beta k_f$ at high pressure, which has been shown to be invalid. If $k_{obsd}^{(2)}$ levels off to a value less than the collision theory value of k_f, then either k_f is less than that value predicted by collision theory, or mechanism I.4 is not a valid representation, or saturation has not really been reached. We see no reliable method for estimating β directly from experimental values of $k_{obsd}^{(2)}$ vs. [M].

When the pressure dependence of k_b is considered, the definitions of low and high pressure change slightly. Recall that k_b is pressure dependent if the microscopic rate constant $k'_b(E,J)$ is dependent on the internal state of the excited complex. Then the limiting pressure regimes are defined by eq V.5,

$$\text{low pressure: } k_c\beta[M] << k'_b(E,J) \quad \text{(V.5a)}$$

$$\text{high pressure: } k_c\beta[M] >> k'_b(E,J) \quad \text{(V.5b)}$$

where the appropriate inequality must hold over the entire manifold of E,J states which are produced in appreciable amounts by the activation process. For complexes produced via ion–molecule collisions $k'_b(E,J)$ may vary by several orders of magnitude, resulting in a corresponding broadening of the transition region. For instance, for the case $\beta = 0.3$ in Figure 3 deviation from linearity is observed as low as about 0.002 torr while approach to saturation does not begin to occur until pressures of about 10–50 torr, resulting in a transition region covering over 4 orders of magnitude.

Bates[12] has pointed out that the pressure dependence of k_b invalidates the use of inverse-pressure plots to obtain estimates of k_f, as has been done by Adams et al.[31] for several reactions of CH_3^+. This method has previously been used by Nielson et al.[32] in the study of the reactions of ammonium ions with ammonia and the methylamines. In a detailed theoretical study Bass et al.[7] have shown that inverse pressure plots can lead to estimates of k_f which are in error by several orders of magnitude, while still appearing consistent with experimental data over a limited pressure range.

When the possible pressure dependence of β is considered and when the radiative stabilization step is included, it becomes more difficult to predict the variation of $k_{obsd}^{(2)}$ with pressure. In fact, this could only be done by choosing some form for the collisional transition probability matrix and actually carrying out a series of calculations for some specific system. A complete study should consider different possible forms for the transition probability matrix and should also include different relative values of k_b and k_r. This work is clearly beyond the scope of this paper.

We believe that the methods used in section II provide reliable upper limits on k_b and k_r. The evaluation of k_r is based on the assumption that the pressure $[M]_{1/2}$, at which $k_{obsd}^{(2)}$ is equal to twice its value at zero pressure, lies within the low-pressure regime; i.e., k_b and k_s have not changed substantially from their low-pressure values and collisional stabilization is negligible compared to dissociation. In Appendix A we show that even if these assumptions fail, the pressure $[M]_{1/2}$ can still be used to provide a valid upper limit on k_r.

The evaluation of $k^{(3)}$ and then k_b from the slope of $k_{obsd}^{(2)}$ vs. [M] is based on the assumption that the corresponding experimental data lies in the low-pressure regime. This assumption is supported by the fact that the experimental data does appear linear in this region. Equation II.1 can be differentiated with respect to $[M]$ to yield

$$\frac{\partial k_{obsd}^{(2)}}{\partial[M]} = \frac{k_f}{(k_b + \beta k_c[M] + k_r)^2}\left\{k_b\left(\beta k_c + k_c[M]\frac{\partial\beta}{\partial M}\right) - \frac{\partial k_b}{\partial[M]}(\beta k_c[M] + k_r)\right\} \quad \text{(V.6)}$$

While it is not at once obvious that linearity results only if the low-pressure conditions are met, it appears unlikely that the expression in eq V.6 will remain constant over some pressure range unless β and k_b are independent of pressure and the $\beta k_c[M]$ term in negligible, in which case

$$\frac{\partial k_{obsd}^{(2)}}{\partial[M]} = \frac{k_f k_b \beta k_c}{(k_b + k_r)^2} \quad \text{(V.7)}$$

If k_r is much smaller than k_b, then eq V.7 yields the same slope as that predicted by eq II.4. Unless it can be shown that some reasonable functional forms for k_b and β_s the slope in eq V.6 remaining constant over a substantial pressure range, we think it reasonable to conclude that a constant slope indicates that low-pressure kinetics are applicable.

When the pressure dependence of β is included, the approach to saturated kinetics may be slower or faster than that predicted assuming β is constant. It is difficult to estimate the expected change since this may depend strongly on the nature of the model used for the collisional transition probability matrix. The definition of high and low pressures becomes a little more involved than that given in eq V.5, which essentially ensures that within the low- or high-pressure regions collisional stabilization and unimolecular decomposition are not competitive with each other over any part of the E,J manifold which is substantially populated. When possible pressure dependence of β, and also k_r, is considered, it is difficult to write a simple expression such as that in eq V.5 as a definition of low and high pressures. Instead, it may be necessary to look at the steady-state distribution function determined from eq III.4 and to define the low- and high-pressure regimes as those in which the distribution function becomes insensitive to further changes in pressure.

It is expected that at high enough pressures collisional stabilization will overwhelm unimolecular decomposition, and $k_{obsd}^{(2)}$ should approach k_f. However, deviations from this behavior may result if the required pressure is very large. Consider an A^+ + B collision for which the centrifugal barrier may be located at a separation large compared to molecular size, say ≥20 Å or so. There is some finite time required for the A^+ + B pair to traverse the distance from the barrier to the region of chemical interaction, say ≤5 Å or so. During this time period there is the possibility that one of the collision partners may undergo a collision with bath gas M and be deflected sufficiently so that the ion–molecule pair never reach the region of chemical interaction. This would result in the actual rate of complex formation being lower than k_f at high pressures. Hence, $k_{obsd}^{(2)}$ would level off to some value less than k_f as saturation was reached.

A rough estimate of the pressure required for the above effect to be substantial can be obtained as follows: This three-body effect will be substantial when the time required for the $CH_3{\cdot}HCN^+$ complex to form is roughly equal to the mean lifetime between $CH_3{\cdot}HCN^+$/He collisions. To estimate the average duration of the CH_3^+ + HCN interaction, we can use 25 Å as the location of the centrifugal barrier and can take the relative velocity of

(31) N. G. Adams, D. Smith, D. G. Lister, A. B. Rakshit, M. Tichy, and N. D. Twiddy, *Chem. Phys. Lett.*, **63**, 166 (1979).
(32) P. V. Neilson, M. T. Bowers, M. Chau, W. R. Davidson, and D. H. Aue, *J. Am. Chem. Soc.*, **100**, 3649 (1978).

approach of the CH_3^+ + HCN pair to be about 4×10^4 cm/s (this corresponds to an energy of $^1/_2kT$ at room temperature). The duration of the CH_3^+ + HCN collision is then about 5×10^{-12} s.. If this is also the mean time between $CH_3{\cdot}HCN^+$/He collisions then [He] $\approx 4 \times 10^{20}$ mol/cm^3, which corresponds to a pressure of about 10^4 torr. Hence, it is unlikely that this process plays any substantial role under ordinary laboratory conditions.

One additional point which we would like to address here is Bates' statement that "use of lifetimes in discussing ion–molecule association should be avoided".[12] Our opinion is that lifetimes are important quantities to consider when discussing ion–molecule association. The lifetime can be used as a rough indication of which types of processes may be operative, of whether or not energy randomization may be expected to occur, and of what pressures may be required to stabilize an appreciable fraction of the complexes formed. We believe that the main point of confusion introduced by Bates is the use of an average lifetime and an average rate constant which are defined independently, with the result that[12]

$$\bar{k}_d\bar{\tau}_d > 1 \tag{V.8}$$

where $\bar{k}_d$ represents the average dissociation rate constant and $\bar{\tau}_d$ is the average lifetime.

However, when we consider the mechanism used by Bates

$$A^+ + B \underset{k_d}{\overset{k_f}{\rightleftharpoons}} (AB^+)^* \begin{cases} \xrightarrow{k_4[M]} AB^+ + M \\ \xrightarrow{k_5[M]} A^+ + B + M \end{cases} \tag{V.9}$$

and the resulting expression for the overall rate constant for the reaction

$$A^+ + B + M \xrightarrow{k_1} AB^+ + M \tag{V.10}$$

given by Bates as

$$k_1 = k_f\bar{\tau}_dk_4[M] \tag{V.11}$$

in the limit that $\bar{k}_d >> (k_4 + k_5)[M]$, it becomes apparent that eq (V.11) is obtained from a steady-state treatment for $(AB^+)^*$ only if the definition

$$\bar{\tau}_d \equiv 1/\bar{k}_d \tag{V.12}$$

is used. Hence, Bates' own introduction of $\bar{\tau}_d$ into the rate expression is based upon the definition in eq V.12 which precludes the possibility he later presents in eq V.8.

We suggest that lifetimes are meaningful quantities to discuss in regard to ion–molecule association reactions. However, when used in kinetic schemes as in the case above, it should be understood that the phrase "average lifetime" actually refers to the "reciprocal of the average rate constant", as in eq V.12.

Finally, we should mention that the approximate value of $k_r = 1.4 \times 10^4$ s^{-1} determined in the current study falls between usual values of vibrational (10^2–10^3 s^{-1}) and electronic ($\geq 10^5$ s^{-1}) emission rates. In fact, it is not at all clear that k_r represents an emission rate constant at all. The CH_3^+/HCN reactant species are both singlets and correlate to a singlet electronic state of the complex—presumably the lowest energy singlet. It is possible that the radiative rate constant k_r represents a curve crossing rate constant to an excited electronic state which then undergoes rapid spontaneous emission of a photon. One such possible state could originate from the "charge-transfer" states that correlate with CH_3/HCN^+ products at infinite separation. These species both have doublet ground states and lead to at least one stable electronic state upon association. This state could be populated by curve crossing from the singlet state associated with CH_3^+/HCN collisions and then rapidly emit a photon. Such a process is enhanced by the fact that the $CH_3{\cdot}HCN^+$ well depth is 4.2 eV, with dissociation to CH_3^+ + HCN the lowest energy pathway.

VI. Summary and Conclusions

The main points of this paper can be summarized as follows.

(1) Application of statistical reaction rate theory to radiative association reactions leads to complicated and time-consuming computations if collisional and radiative transitions are accounte for in detail as in mechanism III.1.

(2) Simplication of the collisional and radiative steps to accour only for average stabilization rates greatly simplifies the com putational procedure. However, this will also tend to obscure th pressure and temperature dependence of the results.

(3) The theoretical model in eq III.7, which uses the simpli fications in 2 above, yields good agreement with experimental dat for the CH_3^+ + HCN association reaction. On the basis c comparisons between theory and experiment, it is estimated tha radiative stabilization of the $(CH_3{\cdot}HCN^+)^*$ intermediate proceed with a rate constant on the order of 10^4 s^{-1} and that collisions wit He gas have a stabilization efficiency in the range from 0.1 t 0.3.

(4) When analyzing experimental results, it should be kept i mind that data which intuitively appears to correspond to the limi of either low- or high-pressure kinetics may, in reality, correspon to pressures substantially removed from these limits. Althoug reasonable rate parameters may be obtained by invoking high or low-pressure kinetics in some cases, there is at least a possibilit that these results are not valid. Also, parameters estimated i one of the limiting pressure regimes are not necessarily applicabl to other pressures.

(5) Lifetimes can be important parameters to discuss in regar to ion-molecule association reactions. When lifetimes are use to characterize various reaction rates, the term "average lifetime should be understood to correspond to the "reciprocal of th average rate contant".

Acknowledgment. This research was supported by Grant CHE77-15499 and CHE80-20464 of the National Scienc Foundation, by Grant PR-180 of the Presidents Fund, Californi Institute of Technology, and by the Jet Propulsion Laboratory California Institute of Technology under Contract No. NAS7-10(sponsored by the National Aeronautics and Space Administratior We gratefully acknowledge these sponsors.

Appendix A

Let $k_{b1/2}$ and $\beta_{1/2}$ represent the values of k_b and β, respectively at the pressure $[M]_{1/2}$ at which $k_{obsd}^{(2)}$ is equal to twice its valu at zero pressure. Then

$$\frac{k_r(\beta_{1/2}k_c[M]_{1/2} + k_r)}{k_{b_{1/2}} + \beta_{1/2}k_c[M]_{1/2} + k_r} = \frac{2k_fk_r}{k_{b_0} + k_r} \tag{A.1}$$

where k_{b_0} is the value of k_b at zero pressure. This is rearrange to

$$k_r = \frac{\beta_{1/2}k_c[M]_{1/2}}{2R - 1} \tag{A.2}$$

where

$$R \equiv \frac{k_{b_{1/2}} + \beta_{1/2}k_c[M]_{1/2} + k_r}{k_{b_0} + k_r} \tag{A.3}$$

Since k_b is expected to increase with pressure, it is apparent tha $R \geq 1$. Since $\beta_{1/2} \leq 1$, it follows that eq A.2 provides a valid upp limit on k_r

$$k_r \leq k_c[M]_{1/2} \tag{A.4}$$

Equation A.4 can be applied by simply estimating $[M]_{1/2}$ fron a plot of experimental data, regardless of whether such a plot i linear or not.

Appendix B. Parameters Used in Calculations

CH_3^+. This ion is expected to be planar and similar in structur to the CH_3 radical.[33] The out-of-plane deformation frequenc is given in the literature,[33] and the remaining frequencies ar estimated. The geometric mean rotational constant is calculate

(33) G. Herzberg, "Molecular Spectra and Molecular Structure", Vol. III VanNostrand, Princeton, NJ, 1967.

from the literature value[33] of the rotational constant about an axis perpendicular to the symmetry axis.

HCN. All parameters are taken directly from the literature.[33]

CH_3·HCN$^+$. The structure[34] is assumed to be CH_3—C≡N$^+$—H. Vibrational frequencies are taken to be those of CH_3—C≡CH,[35] except the C—H and C≡C stretch frequencies are changed to those expected for N—H and C≡N stretches. The rotational constant is calculated from the structure by using the following bond lengths (in Å) C—H (1.0 for —CH_3 group), C—C (1.6), C≡N (1.16), and N—H (1.01) and assuming the methyl group to be tetrahedral and the sketal chain to be linear.

(34) A. Illies, S. Liu, and M. T. Bowers, *J. Am. Chem. Soc.*, in press.

(35) T. Shimanouchi, "Tables of Molecular Vibrational Frequencies", Consolidated Vol. I, National Bureau of Standards, Washington, DC, 1972.

Ground States of Molecules. 58.[1] The C_4H_4 Potential Surface

Herbert Kollmar,[1a] Francisco Carrion, Michael J. S. Dewar,* and Richard C. Bingham[1b]

Contribution from The University of Texas at Austin, Austin, Texas 78712.
Received October 14, 1980

Abstract: The singlet potential surface for C_4H_4 species has been extensively explored, using MINDO/3. It is thought that all local minima corresponding to normal closed shell molecules have been located, together with the transition states for their easiest modes of interconversion. Entry to the C_4H_4 system by the dimerization of acetylene can follow two paths, one involving 3-cyclopropenylcarbene as an intermediate. It is suggested that this reaction is responsible for initiation of detonation in acetylene under pressure or as a solid or liquid.

Cyclobutadiene (**1**) and tetrahedrane (**2**) have long been sought by organic chemists, partly because of their chemical significance but perhaps even more so because of their aesthetic appeal. Cyclobutadiene is the simplest cyclic polyene and as such plays a key role in theories of aromaticity. Tetrahedrane, the simplest of the polyhedranes, should exemplify in a very clear manner the effects of extreme angle strain.

After generations of effort, **1** was finally obtained by Pettit et al.[2] as a reaction intermediate. While **1** itself dimerizes immediately, its spectroscopic properties have been studied by several groups of workers in matrices at low temperatures.[3] Derivatives of **1** containing bulky substituents can exist as stable monomeric species[4,5] and one of these (**3**) has been obtained[5] by rearrangement of **4**, the only known[5] derivative of tetrahedrane.

If **1** is aromatic, it should have a symmetrical square structure with equal bond lengths, whereas if it is antiaromatic, the lengths of the bonds in it should alternate. In the latter case, there is the possibility that a square form of the triplet might represent the ground state. Further points of interest are the stabilities of **1** and **2** relative to one another and to two molecules of acetylene (**5**) and the ease of the "forbidden" interconversions of **1**, **2**, and **5**. In view of the importance of these problems and the lack until very recently of any experimental data concerning them, numerous attempts have been made to solve them by theoretical calculations, both semiempirical[6] and ab initio.[7] The most reliable ab initio

Chart I

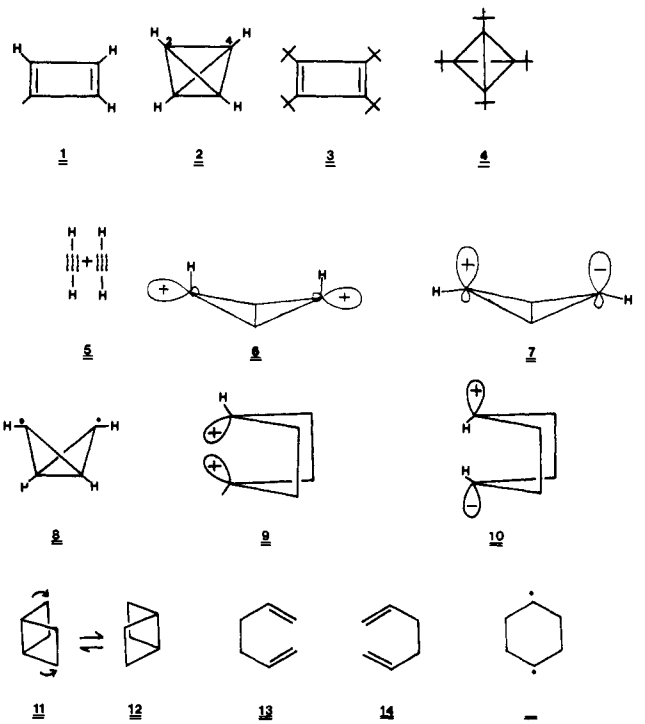

(1) (a) Lehrstuhl fur Theoretische Chemie, der Ruhr-Universitat Bochum, D-4630, Bochum, W. Germany. (b) Dupont Experimental Station, F & F Dept., Bldg. 293, Wilmington, Dela. 19893.

(2) Watts, L.; Fitzpatrick, J. F.; Pettit, R. *J. Am. Chem. Soc.* **1965**, *87*, 3253; **1966**, *88*, 623.

(3) (a) Krantz, A.; Lin, C. Y.; Newton, M. D. *J. Am. Chem. Soc.* **1973**, *95*, 2744. (b) Chapman, O. L.; McIntosh, C. L.; Pacansky, J. *Ibid.* **1973**, *95*, 614. Chapman, O. L.; De LaCruz, D.; Roth, R.; Pacansky, J. *Ibid.* **1973**, *95*, 1337. (c) Masamune, S.; Souto-Bachiller, F. A.; Machiguchi, T.; Bertie, J. E. *Ibid.* **1978**, *100*, 4879.

(4) (a) Kimling, H.; Krebs, A. *Angew. Chem., Int. Ed. Engl.* **1972**, *11*, 932. (b) Maier, G.; Alzenea, A. *Ibid.* **1973**, *12*, 1015. (c) Masamune, S.; Nakamura, N.; Suda, M.; Ona, H. *J. Am. Chem. Soc.* **1973**, *95*, 8481. Delbaere, L. T. J.; James, M. N. G.; Nakamura, N.; Masamune, S. *Ibid.* **1975**, *97*, 1973.

(5) (a) Maier, G.; Pfriem, S.; Schafer, U.; Matusch, R. *Angew. Chem., Int. Ed. Engl.* **1978**, *17*, 520. (b) Irngartinger, H.; Riegler, N.; Malsch, K.-D.; Schneider, K.-A.; Maier, G. *Ibid.* **1980**, *19*, 211. (c) The bond alternation in the ring of **3** is less than that in the other stable derivatives of **1** that have been studied, due to the steric repulsions between the *tert*-butyl groups. These distort **3** out of planarity, part way toward **4**. In **4** itself the repulsions between the *tert*-butyl groups should be small.

(6) (a) Dewar, M. J. S.; Gleicher, G. J. *J. Am. Chem. Soc.* **1965**, *87*, 3255. (b) Dewar, M. J. S.; Kollmar, H. W. *Ibid.* **1975**, *97*, 2933. (c) Dewar, M. J. S.; Komornicki, A. *Ibid.* **1977**, *99*, 6174. (d) Halevi, E. A.; Matsen, F. A.; Welshar, T. L. *Ibid.* **1976**, *98*, 7088. (e) Schweig, A.; Thiel, W. *Ibid.* **1979**, *101*, 4742. (f) Böhm, M. C.; Gleiter, R. *Tetrahedron Lett.* **1978**, 1179.

0002-7863/81/1503-5292$01.25/0